On Phase Transitions in Coupled Map Lattices

Wolfram Just[1] and Frank Schmüser[2]

[1] MRC, Queen Mary / University of London, London, UK
w.just@qmul.ac.uk
[2] IAKS, University of Karlsruhe, Karlsruhe, Germany
schmues@ira.uka.de

Coupled map lattices are a paradigm for studying fundamental questions in spatially extended dynamical systems. Within this tutorial we focus on qualitative changes of the motion which are intimately related with the limit of large system size. Similar to equilibrium phase transitions, such qualitative changes are an ubiquitous feature of dynamical systems with a large number of degrees of freedom. Within the first section of this chapter we present an overview and some phenomenological facts of phase transitions in coupled map lattices. The following two sections describe in some details analytical tools which are useful for understanding phase transition behaviour in dynamical systems beyond plain numerical simulations. In section 2 we explain how coupled map lattices are linked with the canonical equilibrium physics of spin systems when techniques of symbolic dynamics are applied. Using a simple model we explain how coupled map lattices are linked with phase transitions in equilibrium spin models. In the third section we describe an alternative approach in terms of kinetic spin models linking the dynamics of coupled map lattices with equilibrium and nonequilibrium statistical mechanics. We keep our presentation throughout this tutorial entirely elementary and confine the presentation to some basic concepts which are useful for tackling the analysis of phase transitions in extended dynamical systems.

1 Introduction and Overview

The dynamics of spatially extended dynamical systems is a long standing issue in theoretical physics and applied mathematical sciences. Prominent examples with strong emphasis on experimental aspects concern pattern formation out of equilibrium [1]. Due to the boost in the understanding of low–dimensional chaotic motion during the last two decades the emphasis has shifted recently towards the investigation of spatio–temporal dynamics. Unfortunately most of the underlying physical equations of motion like Navier–Stokes or Maxwell–Bloch equations are far too complex for analysing fundamental features beyond straightforward numerical simulations. Since time discrete models have proven to be fruitful in understanding low–dimensional chaos, coupled maps have become a paradigm for the investigation of space–time chaos [2, 3]. While the derivation of time discrete models may be based in principle on Poincaré cross sections such an approach does not apply for models with a spatially continuous variable, i.e. partial differential equations. Thus there still does not exist a satisfactory derivation of coupled map lattices from first principles[3].

Qualitative changes of the dynamical behaviour, i.e. topological changes of the phase space portrait are important and universal features. These changes are called bifurcations [4]. In spatially extended dynamical systems an additional mechanism may cause changes of the motion if the limit of a large number of degrees of freedom is considered. Such transitions share common aspects with equilibrium phase transitions in thermodynamic systems. In any finite canonical equilibrium ensemble the partition sum depends analytically on the parameters, e.g. the temperature. Non–analytic behaviour, i.e. qualitative changes may arise when the limit of infinite system size is considered. In fact, an approximate formal description of such equilibrium phase transitions in terms of a simple Ginzburg Landau theory results in an order parameter equation which displays plain bifurcations (e.g. a pitchfork bifurcation for a homogeneous Ising system). Thus it became to some extent popular to term any type of bifurcation a phase transition (cf. e.g. [5]). Here we pursue a different nomenclature. While bifurcations may occur in any type of dynamical system, regardless of the number of degrees of freedom, there are changes of the dynamics which are absent in any finite size system and which occur only if the limit of infinite system size is considered[4]. In accordance with equilibrium thermodynamics we will call such qualitative changes (proper) phase transitions in order to distinguish these features from plain bifurcations. A formal definition of such a concept may become cumbersome (cf. [6]) and we refrain from giving a mathematical account. However, if one wants to study such aspects from a theoretical perspective the investigation of coupled map lattices is quite useful.

Coupled map lattices are spatio–temporal discrete dynamical systems. Consider a lattice, e.g. a spatially one–dimensional array of sites $\nu \in \{0, 1, \ldots, L-1\}$. On each lattice site consider a continuous variable taken e.g. from an interval $x^{(\nu)} \in I$. Then the state of the system is determined by an L–dimensional vector $\underline{x} = (x^{(0)}, \ldots, x^{(L-1)})$. As for the dynamics on each lattice site a map $f : I \to I$ acts on the corresponding component and the value at time $n+1$ is determined from the state at time $n \in \mathbb{N}_0$ through the action of the map f and a coupling between neighbouring sites, e.g.

[3] Sometimes one claims that numerical integration schemes for partial differential equations yield coupled map lattices. We find such an argument superficial. While integration schemes employ a small spacing between grid points, the lattice constant of coupled map lattices is usually large compared with the observed spatial structures. Thus both schemes focus on different asymptotic regimes.

[4] That means the long time limit and the limit of infinite system size do not commute.

$$x_{n+1}^{(\nu)} = (1-\varepsilon) f\left(x_n^{(\nu)}\right) + \frac{\varepsilon}{2}\left[f\left(x_n^{(\nu-1)}\right) + f\left(x_n^{(\nu+1)}\right)\right] \tag{1a}$$

$$= \Phi_\varepsilon\left[f\left(x_n^{(\nu)}\right), f\left(x_n^{(\nu+1)}\right), f\left(x_n^{(\nu-1)}\right), \ldots\right] \tag{1b}$$

$$= \left(T_\varepsilon(\underline{x}_n)\right)^{(\nu)} \quad . \tag{1c}$$

The coupling shown in eq.(1a) is usually called diffusive coupling. There is no special reason for this choice apart from its simplicity and the hope that numerical features are independent from the particular form of the coupling (cf. [7] for a phenomenological analysis of particular models). The parameter $\varepsilon \in [0,1]$ indicates the strength of the coupling. The factor $(1-\varepsilon)$ is introduced for convenience as it ensures that the dynamics of the coupled map lattice (1a) is confined to the phase space I^L. Eq.(1a) clearly indicates that coupled map lattices may be considered as the composition of two actions, namely the action of the single site map f on each lattice site and a coupling function $\Phi_\varepsilon : I^L \to I$ mediating the interaction as indicated in eq.(1b). Such a formulation also indicates that coupling functions are of course not limited to the case of a diffusive (i.e. nearest neighbour) coupling and that quite different choices are possible. Finally, on an even more abstract level one may consider coupled map lattices just as dynamical systems acting on the phase space I^L, where the L–dimensional map T_ε depends on a coupling parameter in such a way that the choice $\varepsilon = 0$ yields for each component the action of the single site map f (cf. eq.(1c)). Which type of formulation is preferred depends on the particular context. In some cases (e.g. when eqs.(1a) or (1b) are used) one needs in addition the specification of boundary conditions when starting the investigation for finite lattice size. Throughout our exposition we will use periodic boundary conditions $x^{(\nu)} = x^{(\nu+L)}$ since they are quite easy to handle. However, to the best of our knowledge no systematic investigation of the influence of boundary conditions is available in the literature.

The formulation of coupled map lattices in terms of eqs.(1b) or (1c) is quite flexible. Generalisations to spatial lattices of dimension larger than one are obvious, by taking the spatial index ν to enumerate the lattice sites and choosing appropriate coupling functions Φ_ε. There is no need to restrict the dynamical variables $x^{(\nu)}$ to intervals and to confine the full phase space to simple cubes I^L. It is even possible to start from the very beginning with a system on infinite lattices e.g. by considering $\nu \in \mathbb{Z}$. Such an approach, usually used in the mathematical context [8, 9, 10, 11, 6] is advantageous for performing rigorous proofs, although it calls for a careful definition of the dynamical system. Our strategy avoids these technicalities and starts from systems of finite size. The limit $L \to \infty$ will be considered when dynamical quantities have been computed. Thus our approach adopts a physicist's point of view of equilibrium phase transitions. In addition starting with a system of large but finite size directly refers to numerical simulations of space–time chaotic dynamics. Finally the formulation in terms of eq.(1b) or (1c) emphasises the role of different symmetries in the dynamical systems. Translation invariance is the most prominent one and we restrict our analysis to the translation invariant case. The study of dynamical systems with broken translation invariance, e.g. random coupled maps, is a science in its own (cf. e.g. [12] and references therein for aspects linking dynamical systems with glass transitions) and is still at its infancy.

Phase transitions in coupled map lattices are intimately linked with the limit of large system size. The effect of the system size on the dynamics can be demonstrated in terms of numerical simulations. A particularly simple example is given by dynamical systems with global coupling, i.e. when the coupling preserves permutation symmetry. A corresponding coupling function reads

$$\Phi[x^{(\nu)}, x^{(\nu+1)}, x^{(\nu-1)}, \ldots] = x^{(\nu)} + \frac{\varepsilon}{L} \sum_{\mu=0}^{L-1} g(x^{(\mu)} - x^{(\nu)}) \tag{2}$$

where the analytical form of the interaction $g(x)$ depends on the particular model. The apparent simplicity of globally coupled models makes this class attractive for the investigation of fundamental properties of chaotic dynamical systems in the limit of large system size [13]. In fact, globally interacting chaotic maps may display nontrivial correlations even for weak interaction [14], provided the single site map f is structurally unstable [15, 16, 17, 18]. The aspect which concerns us most is the appearance of a phenomenon in strongly coupled models [19] which mimics a phase transition like behaviour. When one considers (structurally stable) chaotic single site maps the weak coupling regime is governed by a "space–time chaotic" state, i.e. a regime where the dynamics at different sites is uncorrelated. At a critical coupling strength ε_c, which depends on the particular choice of the single site map and the interaction function, the synchronised solution, i.e. the state $x_n^{(\nu)} = x_n^{(\mu)}$ for all μ and ν, becomes linearly stable. That transition takes place in any system of finite size L and is just a plain bifurcation. The former "space–time chaotic" state remains as a chaotic saddle yielding a "space–time chaotic" transient dynamics. Such a scenario is in full accordance with features known from low dimensional chaotic systems. But the transient times increase when the system size is increased (cf. figure 1 for an example of globally coupled Bernoulli maps). The observed exponential dependence of the mean transient time on the system size, $T_{\varepsilon,L} \simeq \exp(\alpha_\varepsilon L)$, may be understood in terms of a very simple geometric argument [20]. The synchronised solution $x_n^{(\nu)} = x_n^{(\mu)}$ denotes the diagonal in the phase space I^L. For strong coupling $\varepsilon > \varepsilon_c$ this state is linearly stable and possesses a trapping region such that the dynamics tends towards the synchronised solution once the trapping region is entered[5]. From linear stability considerations the trapping region may be estimated by a cylinder with diameter d aligned along the diagonal in phase space. Its volume is estimated by Dd^{L-1} where D denotes the size of the

[5]In formal terms the trapping region may be defined to be a simply connected open subset of the basin of attraction which contains the synchronised solution.

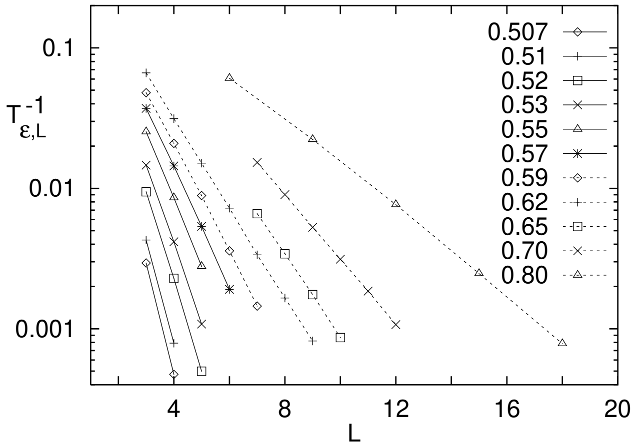

Fig. 1. Dependence of the inverse of the mean transient time (the relaxation rate) on the system size in a globally coupled map lattice for different values of the coupling strength. Confer [19] for further details of the model.

domain I of the single site map f. In the phase space I^L there still exists the "space–time chaotic" saddle causing the chaotic transient dynamics. Assuming some degree of mixing a simple argument tells us that the probability for a typical initial condition to hit the trapping region is given by the volume ratio of the trapping region and the full phase space, Dd^{L-1}/D^L. This crude argument predicts the transient dynamics to be a Poisson process with probability $(d/D)^{L-1}$, i.e. with a time scale being given by $T \simeq (D/d)^L$ (cf. e.g. [19] for some numerical confirmation). Thus exponentially long transients may be explained in terms of simple geometric features, and such arguments may be applied quite generally at least on a phenomenological level. It is just such a property of the transient dynamics which is characteristic for phase transitions. Whereas no stable "nontrivial" dynamics persists in any system of finite size, since finally the synchronised solution is reached, the dynamics stays to be chaotic if systems of large size are considered. Even in models of moderate size L any simulation cannot overcome the transient regime of length $T \simeq \exp(\alpha_\varepsilon L)$. Thus to capture the relevant dynamics in terms of stationary states one has to consider first the limit of large system size and then the asymptotic limit of large time scales. Such a property is quite well known from equilibrium phase transitions[6]. Thus supertransients are an im-

[6]One should however keep in mind that these arguments have to be considered with caution. There are types of transient behaviour, e.g. in diffusive systems, where time scales increase with system size as well, e.g. $T \simeq L^2$. That however usually does not cause phase transitions (cf. e.g. [21]). Thus the simple argument cannot replace a careful formal definition of phase transitions.

portant indicator for the occurrence of phase transitions in spatio–temporal dynamics.

A second class of quite popular examples of coupled map lattices displaying phase transitions are given by spatially two–dimensional coupled systems. The model introduced by Miller and Huse [22] is based on single site maps f of a double tent with an inversion symmetry (cf. figure 2). The single site

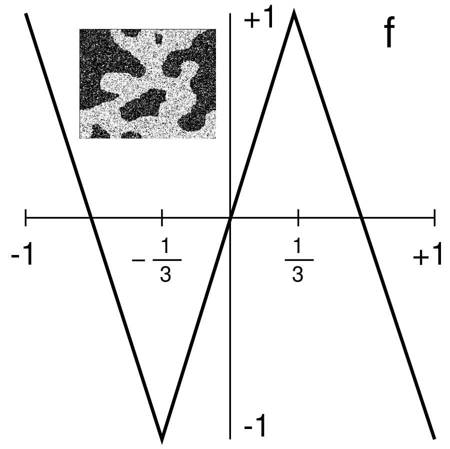

Fig. 2. Single site map of the Miller–Huse model. The inset shows a typical snapshot of pattern appearing in a spatially two–dimensional nearest neighbour coupled Miller–Huse model (black/white pixels encode the sign of the single site variable $x^{(\nu)}$). Confer [22] for further details of the model.

dynamics is chaotic and develops random jumps for the sign $\sigma^{(\nu)} = \mathrm{sign}(x^{(\nu)})$ of the single site variable $x^{(\nu)}$. Thus such a type of motion can be considered as a kind of random spin dynamics, a so called kinetic spin model. Placing the maps on the sites of a two–dimensional square lattice and introducing a nearest neighbour coupling a phase transition appears which shares some common features with the two–dimensional equilibrium Ising model (cf. [23] for the original idea). In fact, numerical simulations of large systems display such a characteristic in a strong coupling regime. But a careful numerical analysis of the critical behaviour shows that naive universality arguments cannot be applied straightforwardly, i.e. the coupled map lattice inherits some hidden long range correlations yielding deviations from the Ising universality class [24, 25]. The description of coupled map lattices in terms of kinetic spin models on some coarse grained level looks promising an we will exploit the analytical structure of such approaches in some detail in section 3.

These two examples indicate what kind of feature one may expect when dealing with phase transitions in coupled map lattices. But solely on numerical grounds it seems difficult to judge whether a particular qualitative change of the dynamics is really related to the limit of infinite system size or whether the phenomenon is just caused by plain bifurcations (cf. e.g. the results in [3]). Therefore phase transitions in coupled map lattices call for formal analytical approaches although one might be forced to restrict the analysis to special model systems.

Already the seemingly simple case of weakly coupled maps poses a considerable challenge. When chaotic single site maps f are considered a naive view suggests that the weakly coupled system $\varepsilon \ll 1$ behaves to some extent like the uncoupled map, e.g. that spatio–temporal correlations decay exponentially and that the statistics of coordinates $x^{(\nu)}$ can be described by some distribution function. But the real proof of such conjectures is far from trivial and requires several technical assumptions concerning the map and the coupling (cf. e.g. [8, 9, 10, 11] for the analysis of various cases). In order to tackle such a problem one assigns symbols lattices to each spatio–temporal pattern. One dimension of the symbol lattice corresponds to the temporal evolution in the dynamical system whereas the other dimensions of the symbol lattice take the spatial extension of the dynamical system into account. Such approaches, called symbolic dynamics in a proper sense, are quite fruitful in linking the ergodic properties of dynamical systems to the statistics of symbol patterns, i.e. to the statistical mechanics of spin systems. In fact, such concepts have been developed in the context of low–dimensional chaos where the corresponding symbolic dynamics yields the statistical mechanics of symbol chains, i.e. one–dimensional spin systems. Then qualitative changes of the dynamics, i.e. bifurcations are reflected by equilibrium phase transitions caused by long range interactions (cf. e.g. [26] for the treatment of intermittent motion). We will consider the essence of such approaches in section 2 using a simple example, so that most of the intricate technical difficulties which enter a more general discussion are avoided. Summarising these ideas, the dynamics of a d–dimensional coupled map lattice is mapped to the equilibrium statistical mechanics of a $d+1$ dimensional spin system. With certain technical assumptions one can show that the case of weakly coupled maps corresponds to the high–temperature phase of the spin system, so that all correlations, i.e. the spatio–temporal correlations in the map lattice, decay exponentially and the invariant measure is unique even in the limit of infinite system size. Increasing the coupling, i.e. decreasing the temperature in the associated spin system, may cause phase transitions when the limit of infinite system size is considered. Thus long range spatio–temporal correlations develop and the dynamical system possesses different ergodic components. One should however keep in mind that this type of approach targets at the limit of infinite system size. The structure of the dynamical system, e.g. the symbolic dynamics must be simple in order to apply the technique.

An alternative approach to deal with phase transitions in dynamical systems keeps the time as a dynamical variable and performs a coarse grained description with respect to the phase space variables only (cf. the discussion of the Miller–Huse model in the previous paragraphs). Based on partitions in phase space, e.g. by assigning at each time n symbols $\sigma_n^{(\nu)}$ according to the sign of $x_n^{(\nu)}$, one obtains a probabilistic model in the symbolic description where the transitions rates between different symbol states are determined by the underlying deterministic dynamics. In such a way one obtains descriptions where on the level of the symbols a time evolution still exists, i.e. a kinetic Ising model or more general a probabilistic cellular automata. Such an idea can be worked out on a quite general level and may be applied to a variety of dynamical systems [27, 28]. But the focus here is on studying coupled map lattices. Application of such a program requires the knowledge of the temporal evolution of the phase space density. Thus one mostly deals with piecewise linear systems where the phase space densities are piecewise constant (cf. e.g. [29] for an investigation of one–dimensional maps or [16, 30] for the treatment of the mean field description of globally coupled maps). Using this property the just mentioned program can be performed explicitly and the dynamics of coupled map lattices may be studied beyond the weak coupling limit [23, 6]. The occurrence of phase transitions in short ranged coupled models seems to require an underlying spatially two–dimensional coupled map lattice in accordance with common wisdom of equilibrium statistical physics. We are devoting section 3 for a more detailed discussion of such fruitful concepts.

There still does not exist a concise picture of phase transitions in spatially extended dynamical systems. At least coupled map lattices are a promising model class to study such a fundamental property. In what follows we will present methods and examples to cope with such a challenge.

2 Symbolic Dynamics of Coupled Maps

Symbolic dynamics is a tool to investigate the temporal evolution in terms of statistical properties of symbol arrays. Using a suitable partition of the phase space each initial condition generates an array of symbols according to the itinerary of the phase space point. Thus the dynamics is mapped to a symbol lattice where the time is translated into one spatial dimension of the lattice. In addition properties of the dynamical system are mapped to the equilibrium statistical mechanics of spin systems when an appropriate Hamiltonian is introduced. Although such approaches are nowadays contained in undergraduate textbooks (cf. e.g. [31, 32]) we try to keep our presentation self–contained and summarise the essential notations in section 2.1. In fact we are not presenting a general theory here but just illustrate the essential features in terms of a simple model, a particular piecewise linear map. We will use this concept to demonstrate in section 2.2 how the dynamics of coupled map lattices can be understood in terms of two–dimensional spin models. In particular, a coupled map lattice will be introduced such that the dynamics is equivalent to the nearest neighbour coupled Ising model. The nature of the phase transition and the consequences for the dynamics of the coupled map lattice is analysed in some detail. For our approach we rely for some technical reasons on the dynamics on invariant sets of saddle type, i.e. repellers. Thus we will in addition recall how such dynamical systems are related with iterated function schemes [33].

2.1 Basic Concepts for Piecewise Linear Maps

We now introduce some fundamental concepts in terms of a simple example, namely a one–dimensional map f which is piecewise linear on an interval, say $I = [-a, a]$ (cf. figure 3). In analytical terms the map is given by

$$f(x) = \begin{cases} g_-(x) & \text{if } x < 0 \\ g_+(x) & \text{if } x > 0 \end{cases} \tag{3}$$

where the two piecewise linear branches of the map are defined by

$$g_-(x) = \begin{cases} \gamma_{--}(x+c) & \text{if } x < -c \\ \gamma_{-+}(x+c) & \text{if } 0 > x > -c \end{cases} \tag{4a}$$

$$g_+(x) = \begin{cases} \gamma_{+-}(x-c) & \text{if } 0 < x < c \\ \gamma_{++}(x-c) & \text{if } x > c \end{cases} \tag{4b}$$

for some fixed value $0 < c < a$ and $\gamma_{\sigma\tilde{\sigma}} > 1$. The map is sketched in figure 3. By construction the map f maps points outside the interval I which are not considered any further, i. e. leave the domain of the map[7]. Points which stay

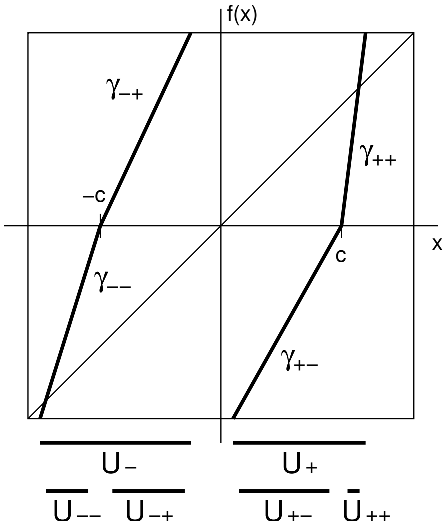

Fig. 3. Diagrammatic view of the map eqs.(3) and (4). The partition (5) and the first generation of cylinder sets is indicated as well.

in the interval I for one iteration are thus located in the two sets U_- and U_+ where

$$U_\sigma = g_\sigma^{-1}(I), \quad \sigma \in \{-,+\} \quad . \tag{5}$$

Phase space points which stay within I upon two iteration steps are contained in one of the intervals $U_{\sigma_0\sigma_1} = g_{\sigma_0}^{-1}(U_{\sigma_1}) = g_{\sigma_0}^{-1}(g_{\sigma_1}^{-1}(I))$ where the symbol

[7]To ensure the structure depicted in figure 3 we suppose that the slopes of the map obey the inequalities $\gamma_{\pm-} > a/(a-c)$ and $\gamma_{\pm+} > c/a$.

string $\sigma_0\sigma_1$ tells us the itinerary of the phase space point with respect to the partition (5). Iterating this procedure we obtain the so called cylinder sets

$$U_{\sigma_0\sigma_1\ldots\sigma_{n-1}} = g_{\sigma_0}^{-1}(U_{\sigma_1\ldots\sigma_{n-1}}) = \{x \in I \,|\, f^k(x) \in U_{\sigma_k},\, 0 \le k \le n-1\} \quad . \tag{6}$$

Taking "the limit" of large n one obtains the invariant set M of the map f, i.e. those phase space points which stay in I for an infinite number of iteration steps

$$M = \bigcap_{n\ge 1} \left(\bigcup_{\sigma_0\ldots\sigma_{n-1}} U_{\sigma_0\sigma_1\ldots\sigma_{n-1}} \right) \quad . \tag{7}$$

Because of the expansiveness of the map f, $|f'(x)| > 1$, the length of the cylinder sets (6) decreases exponentially and the invariant set turns out to be a Cantor set with nontrivial fractal dimension. Since points which are not contained in M will leave the domain of the map our invariant set is of saddle type, i.e. a repelling invariant set.

The labelling of cylinder sets by symbol strings $\sigma_0\sigma_1\ldots\sigma_{n-1}$ has nice properties with respect to the dynamics. Just by definition (6) it follows that

$$f(U_{\sigma_0\sigma_1\ldots\sigma_{n-1}}) = g_{\sigma_0}(U_{\sigma_0\sigma_1\ldots\sigma_{n-1}}) = U_{\sigma_1\ldots\sigma_{n-1}} \tag{8}$$

and

$$f^{-1}(U_{\sigma_1\ldots\sigma_{n-1}}) = \bigcup_{\sigma_0} U_{\sigma_0\sigma_1\ldots\sigma_{n-1}} \tag{9}$$

while unions of cylinder sets obey

$$\bigcup_{\sigma_n} U_{\sigma_0\ldots\sigma_{n-1}\sigma_n} \subseteq U_{\sigma_0\ldots\sigma_{n-1}} \quad . \tag{10}$$

Roughly speaking eq.(8) tells us that the iteration of the map f corresponds to a symbol shift of a symbol string. Fixing an (infinite) symbol sequence $(\sigma_0, \sigma_1, \ldots)$ the corresponding sequence of cylinder sets U_{σ_0}, $U_{\sigma_0\sigma_1}$, $U_{\sigma_0\sigma_1\sigma_2}$, $\ldots$ yields nested intervals which finally single out a unique point $x_{(\sigma_0,\sigma_1,\ldots)} \in M$, since the length of the cylinder sets decreases exponentially. In fact this recipe yields a homeomorphism (i.e. a continuous transformation with a continuous inverse) between the invariant set M and the space of all symbol sequences $\Sigma = \{-,+\}^{\mathbb{N}}$. Due to eq.(8) this transformation nicely complies with the dynamics. Introducing the symbol shift S by $S : (\sigma_0, \sigma_1, \ldots) \mapsto (\sigma_1, \ldots)$ we obviously have $f(x_{(\sigma_0,\sigma_1,\ldots)}) = x_{S(\sigma_0,\sigma_1,\ldots)}$. This property is usually condensed in a commuting diagram[8]

[8]Since we are considering repelling sets our transformation is a conjugacy. Often such a property has to be relaxed. If one considers attracting sets then the relation between phase space points at the boundary of the partition and symbol sequences fails to be uniquely defined.

$$\begin{array}{rcl} S : \Sigma & \longrightarrow & \Sigma \\ \updownarrow & & \updownarrow \\ f : M & \longrightarrow & M \end{array} \quad . \tag{11}$$

Thus the dynamics is equivalent to a symbol shift and orbits of the map f (i.e. initial conditions on the repeller) are efficiently labelled by symbol sequences. Our symbolic dynamics is based on the partition (5) of the phase space. Such partitions are usually called Markov partitions since the corresponding symbol sequences do not contain long ranged correlations between the symbols.

So far the construction has focussed on topological properties of the dynamics. We are now going to address the question “how frequently” a particular orbit, i.e. a symbol sequence, occurs. To be more definite we introduce probabilities for a symbol string $\sigma_0\sigma_1 \ldots \sigma_{n-1}$ to occur when iterating the map f. Since the phase space points generating such a symbol string are contained in the corresponding cylinder set (6), the probabilities may be denoted by $\mu(U_{\sigma_0\sigma_1\ldots\sigma_{n-1}})$ where μ denotes an invariant measure. The condition of time invariance of the probabilities requires that (cf. eq.(9))

$$\mu(U_{\sigma_1\ldots\sigma_{n-1}}) = \mu(f^{-1}(U_{\sigma_1\ldots\sigma_{n-1}})) = \sum_{\sigma_0} \mu(U_{\sigma_0\sigma_1\ldots\sigma_{n-1}}) \tag{12}$$

whereas the usual subadditivity of a measure yields (cf. eq.(10)[9])

$$\mu(U_{\sigma_0\ldots\sigma_{n-1}}) = \sum_{\sigma_n} \mu(U_{\sigma_0\ldots\sigma_{n-1}\sigma_n}) \quad . \tag{13}$$

Finally normalisation requires that

$$1 = \sum_{\sigma} \mu(U_\sigma) \quad . \tag{14}$$

Actually eqs.(12), (13), and (14) just define the invariant measure, and there are many possible solutions of these equations. For instance if we take the ansatz

$$\mu(U_{\sigma_0\ldots\sigma_{n-1}}) = h_{\sigma_0\sigma_1} \frac{p_{\sigma_0\sigma_1}}{\alpha} \frac{p_{\sigma_1\sigma_2}}{\alpha} \ldots \frac{p_{\sigma_{n-3}\sigma_{n-2}}}{\alpha} \nu_{\sigma_{n-2}\sigma_{n-1}} \tag{15}$$

with nonnegative weights $p_{\sigma\tilde{\sigma}} \geq 0$ on the right–hand side, then the condition of invariance (12) results in

$$\alpha h_{\sigma_1\sigma_2} = \sum_{\sigma_0} h_{\sigma_0\sigma_1} p_{\sigma_0\sigma_1} \tag{16}$$

while the subadditivity (13) yields

[9] Since the invariant measure is supported by M, eq.(10) becomes an identity when the cylinder sets are restricted to M.

$$\alpha \nu_{\sigma_0\sigma_1} = \sum_{\sigma_2} p_{\sigma_0\sigma_1} \nu_{\sigma_1\sigma_2} \quad . \tag{17}$$

Eqs.(16) and (17) are nothing else but eigenvalue equations for the 4×4 matrix $A_{\sigma\tilde{\sigma},\tau\tilde{\tau}} = p_{\sigma\tilde{\sigma}}\delta_{\tilde{\sigma}\tau}$ which is usually called the transfer matrix of the map. Actually eq.(16) is just the celebrated Frobenius–Perron equation [34] written with respect to a basis consisting of piecewise constant functions (cf. e.g. [35]). Finally normalisation (14) results in

$$1 = \sum_{\sigma_0\sigma_1} h_{\sigma_0\sigma_1} \nu_{\sigma_0\sigma_1} \quad . \tag{18}$$

Thus given the weights $p_{\sigma\tilde{\sigma}}$ the parameters of the measure are determined[10].

We have computed a whole family of invariant measures where each measure is in fact ergodic. There still remains the problem which measure describes the dynamics of "typical" initial conditions. Since we are dealing with repelling sets, i.e. a Lebesgue typical initial condition leaves the domain of our map after a finite number of iterations, this question deserves a more detailed discussion. If one considers a uniform distribution of initial conditions in the interval I then after n iteration steps the fraction $\sum_{\sigma_0\ldots\sigma_{n-1}} \lambda(U_{\sigma_0\ldots\sigma_{n-1}})$ is still contained in I, where $\lambda(U_{\sigma_0\ldots\sigma_{n-1}})$ denotes the normalised length (i.e. the normalised Lebesgue measure) of the cylinder set. By construction (cf. eq.(8)) the length obeys

$$\lambda(U_{\sigma_0\sigma\ldots\sigma_{n-1}}) = \frac{1}{\gamma_{\sigma_0\sigma_1}} \frac{1}{\gamma_{\sigma_1\sigma_2}} \cdots \frac{1}{\gamma_{\sigma_{n-2}\sigma_{n-1}}} \lambda(U_{\sigma_{n-1}}) \tag{19}$$

since in each iteration step the map f expands by a factor $\gamma_{\sigma\tilde{\sigma}}$. Using this property and some standard transfer matrix argument the fraction of initial conditions remaining in the domain of the map scales exponentially (cf. [36])

$$\sum_{\sigma_0\ldots\sigma_{n-1}} \lambda(U_{\sigma_0\ldots\sigma_{n-1}}) \simeq \alpha^n \tag{20}$$

where the (topological) escape factor $\alpha < 1$ obeys the eigenvalue equations (15) and (16) if the weights are identified with the inverse slopes

$$p_{\sigma\tilde{\sigma}} = \frac{1}{\gamma_{\sigma\tilde{\sigma}}} \quad . \tag{21}$$

Thus the measure (15) determined by the inverse slopes of the map is apparently related with the dynamics of "typical" initial conditions. One may pursue this argument by introducing the concept of conditional invariant measures [37]. Consider a uniform distribution of initial conditions. The fraction

[10] As usual a common factor between the left and the right eigenvector remains undetermined. However, such a fact does not influence the expression of the measure (15).

$\mu_0^c(f^{-1}(I))$ of initial conditions stays in the interval I when performing an iteration step where $\mu_0^c = \lambda$ denotes the (normalised) Lebesgue measure. Therefore $\mu_1^c(E) = \mu_0^c(f^{-1}(E))/\mu_0^c(f^{-1}(I))$ denotes the probability that after one iteration step phase space points appear in the set $E \subseteq I$, provided those initial conditions leaving I are ignored. Iterating this prescription the quantity $\mu_{k+1}^c(E) = \mu_k^c(f^{-1}(E))/\mu_k^c(f^{-1}(I))$ yields the fraction of initial conditions, ending up in E after $k+1$ iteration steps. Using $\mu_0^c(f^{-1}(I)) = \sum_\sigma \lambda(U_\sigma)$, eq.(9) and eq.(19), straightforward iteration results in

$$\begin{aligned}\mu_{k+1}^c(U_{\sigma_0\ldots\sigma_{n-1}}) &= \frac{\sum\limits_{\sigma_{-k-1}\ldots\sigma_{-1}} \mu_0^c(U_{\sigma_{-k-1}\ldots\sigma_{-1}\sigma_0\ldots\sigma_{n-1}})}{\sum\limits_{\sigma_{-k}\ldots\sigma_0} \mu_0^c(U_{\sigma_{-k}\ldots\sigma_0})} \\ &= \frac{\sum\limits_{\sigma_{-k-1}\ldots\sigma_{-1}} \gamma^{-1}_{\sigma_{-k-1}\sigma_{-k}}\cdots\gamma^{-1}_{\sigma_{-1}\sigma_0}\lambda(U_{\sigma_0\ldots\sigma_{n-1}})}{\sum\limits_{\sigma_{-k}\ldots\sigma_0} \gamma^{-1}_{\sigma_{-k}\sigma_{-k+1}}\cdots\gamma^{-1}_{\sigma_{-1}\sigma_0}\lambda(U_{\sigma_0})} \quad . \end{aligned} \tag{22}$$

Standard arguments of linear algebra[11] tell us that the limit

$$h_{\sigma_0\sigma_1} = \lim_{k\to\infty} \frac{\sum\limits_{\sigma_{-k-1}\ldots\sigma_{-1}} \gamma^{-1}_{\sigma_{-k-1}\sigma_{-k}}\cdots\gamma^{-1}_{\sigma_{-1}\sigma_0}}{\sum\limits_{\sigma_{-k}\ldots\sigma_0} \gamma^{-1}_{\sigma_{-k}\sigma_{-k+1}}\cdots\gamma^{-1}_{\sigma_{-1}\sigma_0}\lambda(U_{\sigma_0})} \tag{23}$$

exists since the numerator behaves like $\alpha^k h_{\sigma_0\sigma_1}$ and the denominator like α^k where α denotes the largest eigenvalue and $h_{\sigma_0\sigma_1}$ the corresponding and properly normalised eigenvector of the eigenvalue equation (16) with the choice (21). Thus taking the limit $k \to \infty$ we obtain the stationary probabilities (the so called conditional invariant measure)

$$\mu_\infty^c(U_{\sigma_0\ldots\sigma_{n-1}}) = h_{\sigma_0\sigma_1}\lambda(U_{\sigma_0\ldots\sigma_{n-1}}) \quad . \tag{24}$$

Eq.(24) determines the probability distribution of phase space points when the density is properly rescaled after each iteration step, taking the loss of probability into account. The right–hand side tells us that such a probability is described in terms of a density function where the density is determined by the eigenvalue problem (16) with the special choice (21). In this sense the invariant measure (15) subjected to the choice (21) describes the distribution of typical initial conditions, while the adjoint eigenvalue problem (17) takes the fractal support of the measure into account [38]. Measures which describe

[11] Using e.g. the previously mentioned transfer matrix $A_{\sigma\tilde\sigma,\tau\tilde\tau} = \gamma^{-1}_{\sigma\tilde\sigma}\delta_{\tau\tilde\tau}$ (cf. eqs.(16) and (17)), the numerator and denominator can be expressed in terms of the kth power of this transfer matrix.

the ergodic properties with respect to typical initial conditions are usually called SRB measures. In general they are linked with the local expansion rates as expressed by the fundamental relation (21). Henceforth we will restrict our analysis to this choice. There exists a whole multifractal industry analysing the implications of the other cases and we refer the interested reader to the literature [39, 40, 41].

Properties of the dynamical system, e.g. mean values and correlation functions can be evaluated in terms of the invariant measure (15). If we consider for the purpose of illustration the simplest case, i.e. a piecewise constant observable $G(x) = G_\sigma$ if $x \in U_\sigma$, then the mean value is given by

$$\begin{aligned}\langle G \rangle &= \int G(x)\, d\mu = \sum_\sigma G_\sigma \mu(U_\sigma) \\ &= \frac{1}{n} \sum_{k=0}^{n-1} \sum_{\sigma_0 \ldots \sigma_{n-1}} G_{\sigma_k} \mu(U_{\sigma_0 \ldots \sigma_{n-1}})\end{aligned} \tag{25}$$

where for the last expression we have employed the conditions of invariance eqs.(12) and (13)[12]. For the temporal correlation function one obtains in the same way

$$\begin{aligned}\langle G(x) G(f^\ell(x)) \rangle &= \int G(x) G(f^\ell(x))\, d\mu = \sum_{\sigma_0 \ldots \sigma_\ell} G_{\sigma_0} G_{\sigma_\ell} \mu(U_{\sigma_0 \ldots \sigma_\ell}) \\ &= \frac{1}{n} \sum_{k=0}^{n-1} \sum_{\sigma_0 \ldots \sigma_{n+\ell-1}} G_{\sigma_k} G_{\sigma_{k+\ell}} \mu(U_{\sigma_0 \ldots \sigma_{n+\ell-1}}) \quad .\end{aligned} \tag{26}$$

Inspecting eqs.(25) and (26) the average values can be expressed as canonical equilibrium averages of a single spin variable G_σ when one defines the spin Hamiltonian through the statistical weight

$$\mu(U_{\sigma_0 \ldots \sigma_{n-1}}) = \exp(-H_{\sigma_0 \ldots \sigma_{n-1}}) \quad . \tag{27}$$

The Hamiltonian $H_{\sigma_0 \ldots \sigma_{n-1}}$ defines the statistical mechanics of a spin chain where the spatial extension corresponds to the temporal evolution of the dynamical system. For our model (15) and (21) the Hamiltonian reads

$$\begin{aligned}H_{\sigma_0 \ldots \sigma_{n-1}} &= -\ln h_{\sigma_0 \sigma_1} - \ln \nu_{\sigma_{n-2} \sigma_{n-1}} + \sum_{k=0}^{n-2} \ln \gamma_{\sigma_k \sigma_{k+1}} + (n-2) \ln \alpha \\ &\simeq \sum_{k=0}^{n-1} (-J \sigma_k \sigma_{k+1} - h \sigma_k) + n \ln \alpha\end{aligned} \tag{28}$$

[12] Actually the last expression is useful if one wants to generalise the considerations to more complicated variables where the limit of a fine partition is really needed.

where $4J = -\ln[\gamma_{++}\gamma_{--}/(\gamma_{+-}\gamma_{-+})]$, $2h = -\ln[\gamma_{++}/\gamma_{--}]$, and we use the symbols σ_k as well to indicate the spin quantum number ± 1. Thus apart from boundary conditions which have been omitted in the last line of eq.(28) the Hamiltonian is given by the nearest neighbour coupled Ising chain. The exchange constant is determined by the curvature of the map, the external field by the symmetry, and the ground state energy by the escape rate.

So far the formulation of ergodic averages in terms of canonical ensembles is just a formal procedure. It does not help to compute the dynamical properties since the invariant measure must be known a priori in order to determine the Hamiltonian. But standard results of statistical mechanics tell us how the mean values and the correlations depend on the parameters of the Hamiltonian, i.e. on the parameters of the map. Such results are in particular valid in the thermodynamic limit $n \to \infty$, i.e. in the limit of fine partitions of the phase space. Since we have obtained a spin chain with short range interactions canonical averages are analytic expressions and the correlations decay exponentially, even if quite complicated observables $G(x)$ are considered. Thus we obtain that the mean value (25) depends analytically on the parameters of the map and that the correlation (26) decays exponentially. Summarising, by adopting a symbolic description and translating the time into a lattice dimension dynamical properties may be reformulated within the concepts of canonical equilibrium statistical mechanics. For expansive dynamical systems we obtain Hamiltonians with short range interaction. No (equilibrium) phase transitions occur and analytic dependence of the mean values on the parameters of the system is obtained. If expansiveness is violated then long range interactions are caused and phase transitions may occur. A prominent example is intermittent dynamics where the bifurcations in the dynamical system are mapped to particular phase transitions in the corresponding equilibrium statistical mechanics [26].

A direct numerical simulation of our model is not feasible since Lebesgue almost all initial conditions leave the domain I. But considering the "inverse" dynamics in terms of an iterated function scheme [33] we obtain a nice method to generate a time series and to compute the invariant density by numerical means. In fact such an approach just formalises the construction of the invariant set M, eq.(7), by a sequence of cylinder sets. Starting with our initial domain $E_0 = I$ the preimage $E_1 = f^{-1}(E_0) = \cup_\sigma g_\sigma^{-1}(E_0)$ consists of the two intervals (5). We may iterate such a procedure $E_{k+1} = \cup_\sigma g_\sigma^{-1}(E_k)$ so that E_k consists of the union of cylinder sets of order k. Since our original map is expansive the inverse branches g_σ^{-1} are contractions and the sequence (E_k) converges towards the (maximal) invariant set M of our dynamical system. It is determined by the condition (cf. e.g. [33] for a nice introduction containing the technical details)

$$M = \bigcup_\sigma g_\sigma^{-1}(M) \quad . \tag{29}$$

The collection of contractions $\{g_\sigma^{-1}\}$ is called an iterated function scheme. We may apply this idea to generate orbits of our dynamical system. Suppose the symbol sequence $(\sigma_0, \sigma_1, \ldots)$ of an orbit is given. Then the orbit obeys $x_{n+1} = f(x_n) = g_{\sigma_n}(x_n)$. Inversion of the branch yields the reversed dynamics $x_n = g_{\sigma_n}^{-1}(x_{n+1})$. Since the inverse branches are contractions, any initial value converges after a short transient phase towards the true orbit. Of course in order to generate a "typical" orbit (i.e. to take a "typical" symbol sequence) one has to formulate the concept of an invariant measure using the iterated function scheme. By definition the invariant measure obeys

$$\mu(E) = \mu(f^{-1}(E)) = \bigcup_\sigma \mu(g_\sigma^{-1}(E)) \tag{30}$$

for any (measurable) set E. In order to generate a μ–typical symbol sequence we consider the conditional probability that a symbol σ_n appears provided that the symbols σ_k, $k \geq n+1$ are given

$$w(\sigma_n|\sigma_{n+1}, \sigma_{n+2}, \ldots) = \lim_{k\to\infty} \frac{\mu(U_{\sigma_n \sigma_{n+1} \ldots \sigma_k})}{\mu(U_{\sigma_{n+1} \ldots \sigma_k})} \quad . \tag{31}$$

Choosing symbols according to these transition probabilities we generate a μ–typical orbit through

$$x_n = g_{\sigma_n}^{-1}(x_{n+1}) \quad \text{with probability } w(\sigma_n|\sigma_{n+1}, \sigma_{n+2}, \ldots) \tag{32}$$

where the symbols σ_k, $k \geq n+1$ are determined by x_k. Such a type of stochastic model yields a typical orbit on our repeller. For our particular case (15) the transition probabilities yield a Markov chain since evaluation of eq.(31) results in

$$w(\sigma_n|\sigma_{n+1}, \sigma_{n+2}, \ldots) = \frac{h_{\sigma_n \sigma_{n+1}}}{h_{\sigma_{n+1} \sigma_{n+2}}} \frac{p_{\sigma_n \sigma_{n+1}}}{\alpha} \tag{33}$$

and the eigenvector $h_{\sigma_{n+1}\sigma_{n+2}}$ does not depend on the second symbol (cf. eq.(16)). The dynamical system (32) admits a skew product structure. The stochastic part may be considered as a single spin flip dynamics with short term memory. The iteration rule for the phase space point x_n is then derived from the dynamics of the symbols.

The invariant measure may be computed in terms of a histogram from a typical trajectory. Since our dynamical system is supported by a fractal no smooth density exist and visualisation calls for a cumulative distribution, e.g. $P_<(x) = \mu((-\infty, x])$. If one considers the simplest case, i.e. linear contractions g_σ^{-1}, then the cumulative distribution clearly shows a devil's staircase like behaviour and thus reflects the Cantor set structure of the invariant set (cf. figure 4). Introducing a finite external field into the corresponding statistical mechanics breaks the symmetry of the map and the invariant measure. If we introduce a finite curvature in the branches of the map, i.e. if we take

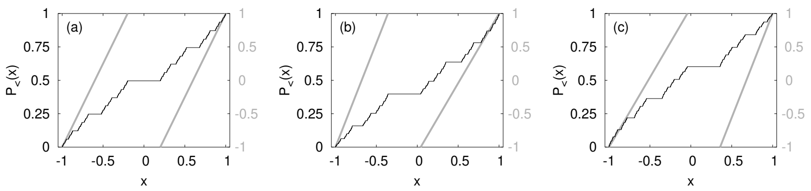

Fig. 4. Cumulative distribution $P_<(x)$ of a piecewise linear model with $J = 0$ and (a) $h = 0$, (b) $h = 0.2$, and (c) $h = -0.2$ (cf. eq.(28)). In each case the escape factor is chosen to be $\alpha = 0.8$. The shape of the single site map f is sketched in grey.

a finite nearest neighbour interaction in the statistical mechanics into account no qualitative change occur. However, in the low temperature limit, i.e. $J \to \infty$, a singular point is approached since the decay of equilibrium correlation functions of the nearest neighbour Ising model slows down. We may study how this behaviour is reflected by the dynamical system. There are in fact different ways approaching the asymptotic limit, depending on the behaviour of the ground state energy, i.e. the escape factor. Figure 5 summarises some typical results. One clearly recognises that the cumulative

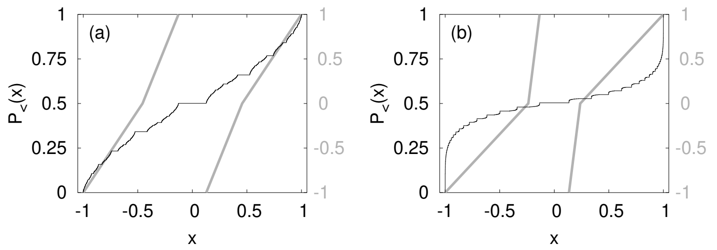

Fig. 5. Cumulative distribution $P_<(x)$ of a piecewise linear model with $h = 0$ and (a) $J = 0.25$, (b) $J = 1.0$ (cf. eq.(28)). In each case the escape factor is chosen to be $\alpha = 0.8$. The shape of the single site map f is displayed in grey.

distribution develops a square root like singularity at the fixed points of the map, $x = \pm 1$. Thus the invariant measure accumulates in this phase space region. The neighbourhood of the fixed point generates symbol sequences containing long strings of symbols with the same sign, i.e. the fixed points corresponds to the ground states of the Ising Hamiltonian. Furthermore since the fixed points tend to become marginally stable in the limit $J \to \infty$ the decay of temporal correlations slows down. Thus the behaviour is a caricature of the intermittency transition mentioned previously [26, 41]. The two pure phases correspond to the two fixed points of the map and the invariant measure tends to localise at the fixed points. Of course no phase transition is caused since we have considered a degenerated limit.

In summary, low–dimensional dynamical systems have been cast into the framework of canonical equilibrium statistical mechanics of spin chains. In this approach the spatial coordinate of the spin system corresponds to the temporal evolution of the dynamical system. Since the invariant measure defines the spin Hamiltonian, the explicit construction of the statistical mechanics requires the full solution of the dynamical model. One may generalise these concepts to more complicated dynamical systems, e.g. higher dimensional expanding maps [42]. The crucial step for the application of the present concept is the knowledge of the underlying symbolic dynamics (cf. e.g. [43]). Since our focus is on fundamental aspects in coupled map lattices we stay with our simple model. For the statistical mechanics of general low–dimensional dynamical systems we refer the interested reader to the literature [44].

2.2 Coupled Repeller Maps

Based on the approach sketched in section 2.1 we are going to introduce a coupled map lattice exhibiting an Ising–like phase transition. Our construction closely follows the elementary ideas of [45]. Consider a spatially one–dimensional lattice of length L and place on each lattice site the single site map (3). To introduce the essential notation let us first consider the trivial case without coupling, $\Phi_{\varepsilon=0}[x^{(\nu)},\ldots] = x^{(\nu)}$. Then the dynamics is governed by

$$x_{n+1}^{(\nu)} = (T_{\varepsilon=0}(\underline{x}_n))^{(\nu)} = f(x_n^{(\nu)}) \quad . \tag{34}$$

On each lattice site a symbol $\sigma^{(\nu)} \in \{-,+\}$ indicates which branch (4) of the single site map is applied. Actually the uncoupled map (34) is not defined on the full phase space I^L since points leave the domain on iteration. The partition (5) of the single site map carries over to a partition of the spatially extended system in the trivial way

$$U_{\underline{\sigma}} = U_{\sigma^{(0)}} \times U_{\sigma^{(1)}} \times \ldots \times U_{\sigma^{(L-1)}} \quad . \tag{35}$$

The symbol sequence $\underline{\sigma} = (\sigma^{(0)}, \sigma^{(1)}, \ldots, \sigma^{(L-1)})$ which labels the set (35) takes the spatial degrees of freedom into account. Each set is mapped to I^L by the system $T_{\varepsilon=0}$. To take the temporal aspects of the motion into account we again introduce finer partitions of the phase space in terms of cylinder sets. Since we consider still the uncoupled case the cylinder sets are given by direct products of the single site quantities

$$U_{\underline{\sigma}_0\underline{\sigma}_1\cdots\underline{\sigma}_{n-1}} = \{\underline{x} \in I^L \,|\, T_{\varepsilon=0}^k(\underline{x}) \in U_{\underline{\sigma}_k}, 0 \le k \le n-1\} \quad . \tag{36}$$

Obviously the cylinder sets are linked with the dynamics through the property (cf. eq.(8))

$$T_{\varepsilon=0}(U_{\underline{\sigma}_0\underline{\sigma}_1\cdots\underline{\sigma}_{n-1}}) = U_{\underline{\sigma}_1\cdots\underline{\sigma}_{n-1}} \tag{37}$$

These geometric features are summarised in figure 6. In particular, the product structure of the cylinder sets reflects the fact that our dynamical system possesses no spatial coupling. Cylinder sets, i.e. roughly speaking the space time orbits, are labelled by two–dimensional spin lattices $\underline{\sigma}_0\underline{\sigma}_1 \ldots \underline{\sigma}_{n-1}$. One dimension of the spin lattice corresponds to the temporal evolution whereas the second dimension takes the spatial extension of the dynamical system into account.

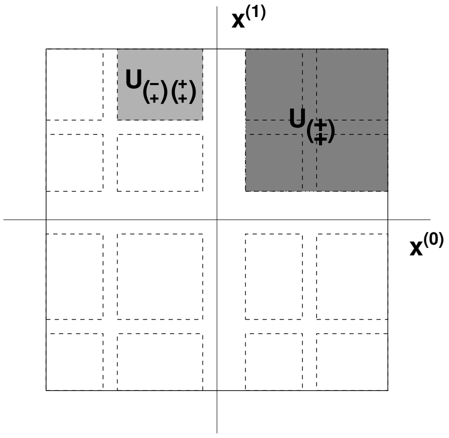

Fig. 6. Diagrammatic view of the first generation of cylinder sets (dashed rectangles) of the uncoupled map lattice (34) for $L = 2$. A cylinder set $U_{\underline{\sigma}\,\underline{\tilde{\sigma}}}$ and its image $U_{\underline{\tilde{\sigma}}}$ are greyshaded.

The invariant measure (15) of the single site map carries over to our dynamical system as well. Using the condition (21) we have

$$\mu_{\varepsilon=0}(U_{\underline{\sigma}_0\underline{\sigma}_1\cdots\underline{\sigma}_{n-1}}) = h_{\underline{\sigma}_0\underline{\sigma}_1} \frac{p_{\underline{\sigma}_0\underline{\sigma}_1}}{\alpha} \frac{p_{\underline{\sigma}_1\underline{\sigma}_2}}{\alpha} \cdots \frac{p_{\underline{\sigma}_{n-3}\underline{\sigma}_{n-2}}}{\alpha} \nu_{\underline{\sigma}_{n-2}\underline{\sigma}_{n-1}} \tag{38}$$

where the weights are defined in terms of the Jacobian $DT_{\varepsilon=0}$ of the uncoupled map

$$p_{\underline{\sigma}\,\underline{\tilde{\sigma}}} = \prod_{\nu=0}^{L-1} \frac{1}{\gamma_{\sigma^{(\nu)}\tilde{\sigma}^{(\nu)}}} = \left|\det\left(DT_{\varepsilon=0}(\underline{x})|_{\underline{x}\in U_{\underline{\sigma}\,\underline{\tilde{\sigma}}}}\right)\right|^{-1} \quad . \tag{39}$$

The remaining quantities entering the invariant measure (38) are likewise given as products of the single site quantities and are thus determined by the associated eigenvalue problem[13] (cf. eqs.(16) and (17))

$$\alpha h_{\underline{\sigma}_1\underline{\sigma}_2} = \sum_{\underline{\sigma}_0} h_{\underline{\sigma}_0\underline{\sigma}_1} p_{\underline{\sigma}_0\underline{\sigma}_1} \tag{40a}$$

$$\alpha \nu_{\underline{\sigma}_0\underline{\sigma}_1} = \sum_{\underline{\sigma}_2} p_{\underline{\sigma}_0\underline{\sigma}_1} \nu_{\underline{\sigma}_1\underline{\sigma}_2} \quad . \tag{40b}$$

---

[13] In general, the largest eigenvalue scales exponentially with the system size, i.e. $\sqrt[L]{\alpha}$ tends to a finite value in the thermodynamic limit.

Following the spirit of the previous section we can rewrite the measure (38) in terms of a canonical weight of a two–dimensional spin Hamiltonian (cf. eq.(28))

$$\begin{aligned} & H_{\underline{\sigma}_0\underline{\sigma}_1\cdots\underline{\sigma}_{n-1}} \\ &= -\ln\mu_{\varepsilon=0}(U_{\underline{\sigma}_0\underline{\sigma}_1\cdots\underline{\sigma}_{n-1}}) \\ &= -\ln h_{\underline{\sigma}_0\underline{\sigma}_1} - \ln\nu_{\underline{\sigma}_{n-2}\underline{\sigma}_{n-1}} + \sum_{k=0}^{n-2}\sum_{\nu=0}^{L-1}\ln\gamma_{\sigma_k^{(\nu)}\sigma_{k+1}^{(\nu)}} + (n-2)L\ln\alpha \quad . \end{aligned} \tag{41}$$

Thus we obtain the statistical mechanics of uncoupled spin chains. The particular boundary conditions are again determined by the eigenvectors of the transfer matrix. No phase transition will occur in this model. But we suspect that the corresponding two–dimensional spin Hamiltonian may exhibit equilibrium phase transitions when a spatial coupling is introduced in the coupled map lattice. Hence the dynamical system may develop different ergodic components in the thermodynamic limit.

In order to introduce a nearest neighbour coupling, while keeping the symbolic dynamics as simple as possible, we consider a piecewise linear coupled map lattice where the local slopes depend on the neighbouring symbols. A simple model is obtained when an unidirectional coupling with periodic boundary conditions $x^{(L)} = x^{(0)}$ is considered. Using the abbreviations (cf. eq.(28))

$$\Gamma_{\sigma^{(\nu)}\tilde{\sigma}^{(\nu)}\sigma^{(\nu+1)}} = \exp(-h\sigma^{(\nu)} - J\sigma^{(\nu)}(\tilde{\sigma}^{(\nu)} + \sigma^{(\nu+1)}) + e_0) \tag{42}$$

and (cf. eq.(4))

$$G_{-\sigma}(x) = \begin{cases} \Gamma_{--\sigma}(x+c) & \text{if } x < -c \\ \Gamma_{-+\sigma}(x+c) & \text{if } -c < x < 0 \end{cases} \tag{43a}$$

$$G_{+\sigma}(x) = \begin{cases} \Gamma_{+-\sigma}(x-c) & \text{if } 0 < x < c \\ \Gamma_{++\sigma}(x-c) & \text{if } c < x \end{cases} \tag{43b}$$

we define the coupled map lattice by[14]

$$(T_\varepsilon(\underline{x}))^{(\nu)} = \begin{cases} G_{--}(x^{(\nu)}) & \text{if } x^{(\nu)} < 0 \text{ and } x^{(\nu+1)} < 0 \\ G_{-+}(x^{(\nu)}) & \text{if } x^{(\nu)} < 0 \text{ and } x^{(\nu+1)} > 0 \\ G_{+-}(x^{(\nu)}) & \text{if } x^{(\nu)} > 0 \text{ and } x^{(\nu+1)} < 0 \\ G_{++}(x^{(\nu)}) & \text{if } x^{(\nu)} > 0 \text{ and } x^{(\nu+1)} > 0 \end{cases} \quad . \tag{44}$$

Eq.(44) is essentially the single site map (3) with the local slope depending on the sign of the right neighbour coordinate. The interaction is mediated by the parameter J (cf. eq.(42)) but we still keep the symbol $T_{\varepsilon=J}$ for the

[14]It is still possible to cast the coupled map lattice in the form (1b). But we refrain from writing down the coupling function explicitly.

coupled map lattice in order to be consistent with the notation introduced in section 1. The partition on which the coupled map lattice is defined is now given by (cf. eq.(35))

$$V_{\underline{\sigma}} = G^{-1}_{\sigma^{(0)}\sigma^{(1)}}(I) \times G^{-1}_{\sigma^{(1)}\sigma^{(2)}}(I) \times \ldots \times G^{-1}_{\sigma^{(L-1)}\sigma^{(0)}}(I) \tag{45}$$

and the corresponding cylinder sets read (cf. eq.(36))

$$V_{\underline{\sigma}_0\underline{\sigma}_1\cdots\underline{\sigma}_{n-1}} = \{\underline{x} \in I^L \,|\, T^k_\varepsilon(\underline{x}) \in V_{\underline{\sigma}_k}, 0 \leq k \leq n-1\} \quad . \tag{46}$$

To distinguish between the quantities of the uncoupled and the coupled map lattice we use the symbol V for the sets of the latter model. Of course the dynamical constraint (37) is again valid if the quantities of the coupled map lattice are considered. A diagrammatic view of the cylinder sets is shown in figure 7. Due to the finite coupling the product structure of the cylinder sets is removed.

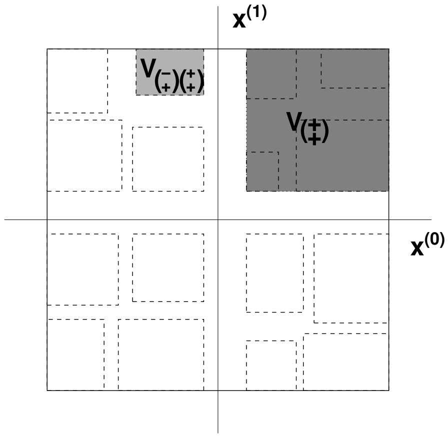

Fig. 7. Diagrammatic view of the first generation of cylinder sets (dashed rectangles) of the coupled map lattice (44) for $L = 2$. A cylinder set $V_{\underline{\sigma}\,\underline{\tilde{\sigma}}}$ and its image $V_{\underline{\tilde{\sigma}}}$ are greyshaded. Cf. figure 6 for the case without coupling.

Since the map lattice T_ε is piecewise linear, the Jacobian yields

$$\begin{aligned}
&\left|\det(DT_\varepsilon(\underline{x})|_{\underline{x}\in V_{\underline{\sigma}\,\underline{\tilde{\sigma}}}}\right| \\
&= \prod_{\nu=0}^{L-1} \Gamma_{\sigma^{(\nu)}\tilde{\sigma}^{(\nu)}\sigma^{(\nu+1)}} \\
&= \exp\left(-h\sum_{\nu=0}^{L-1}\sigma^{(\nu)} - J\sum_{\nu=0}^{L-1}\sigma^{(\nu)}(\tilde{\sigma}^{(\nu)} + \sigma^{(\nu+1)}) + Le_0\right) \quad .
\end{aligned} \tag{47}$$

The invariant measure of our model is given by (cf. eq.(38))

$$\mu_\varepsilon(V_{\underline{\sigma}_0\underline{\sigma}_1\cdots\underline{\sigma}_{n-1}}) = h_{\underline{\sigma}_0\underline{\sigma}_1}\frac{p_{\underline{\sigma}_0\underline{\sigma}_1}}{\alpha}\frac{p_{\underline{\sigma}_1\underline{\sigma}_2}}{\alpha}\cdots\frac{p_{\underline{\sigma}_{n-3}\underline{\sigma}_{n-2}}}{\alpha}\nu_{\underline{\sigma}_{n-2}\underline{\sigma}_{n-1}} \tag{48}$$

where the weight is determined by the inverse of the local expansion rate (cf. eq.(21)), i.e.

$$p_{\underline{\sigma}\underline{\tilde{\sigma}}} = \frac{1}{\left|\det(DT_\varepsilon(\underline{x})|_{\underline{x}\in V_{\underline{\sigma}\,\underline{\tilde{\sigma}}}})\right|} \tag{49}$$

and the corresponding eigenvalue problem (40) determines the remaining parameters of the measure (48). By construction the corresponding Hamiltonian of the two–dimensional symbol lattice is now given by

$$\begin{aligned} & H_{\underline{\sigma}_0\underline{\sigma}_1\cdots\underline{\sigma}_{n-1}} \\ &= -\ln\mu_\varepsilon(V_{\underline{\sigma}_0\underline{\sigma}_1\cdots\underline{\sigma}_{n-1}}) \\ &\simeq \sum_{k=0}^{n-1}\sum_{\nu=0}^{L-1}\left(-h\sigma_k^{(\nu)} - J\sigma_k^{(\nu)}(\sigma_{k+1}^{(\nu)} + \sigma_k^{(\nu+1)})\right) + nL(e_0 + \ln\sqrt[L]{\alpha}) \quad . \end{aligned} \tag{50}$$

Thus we end up with a nearest neighbour coupled two–dimensional Ising model. For $h = 0$ this model displays a second order phase transition at $J_c = \text{Artanh}(\sqrt{2} - 1)$ in the thermodynamic limit. The equilibrium correlations become long ranged, a macroscopic magnetisation appears, and the canonical distribution develops two different ergodic components. These properties are shared by the underlying coupled map lattice. Hence the spatio–temporal correlations do not decay exponentially (cf. eq.(26)) and the time average of $\sum_{\nu=0}^{L-1}\sigma^{(\nu)}/L$ remains finite in the thermodynamic limit (cf. eq.(25)) despite the fact that any finite system coupled map lattice still has a mixing dynamics. The two different ergodic components which develop at the phase transition point just correspond to the pure phases of positive and negative magnetisation, i.e. to trajectories which on average tend to localise either in the left–hand or the right–hand part of the interval I. The ground state of the Hamiltonian (50), i.e. the zero temperature configuration, is given by the fully aligned spin lattice (for $J > 0$). These spin lattices correspond to the two spatially homogeneous fixed points of the map lattice. Thus the phase transition is a macroscopic localisation of the measure at the linearly unstable fixed points. In this respect the coupled map lattice shares some common features with the dynamics of the single site map (cf. section 1). But for the coupled map lattice it is remarkable that the involved fix points are not marginally stable at the phase transition point and throughout the low–temperature phase. A modulation of the local slope by a factor of four is already sufficient to induce the phase transition.

In principle it is even possible to analyse our model by direct numerical simulations despite we are dealing with repelling sets. As already indicated in section 1 the motion on repelling sets can be generated by an iterated function scheme which is determined by the inverse branches of the coupled map lattice determine. The transition probabilities to generate a state $\underline{\sigma}_n$ provided the history $\underline{\sigma}_k$, $k \geq n+1$ is given read (cf. eq.(31))

$$w(\underline{\sigma}_n|\underline{\sigma}_{n+1},\underline{\sigma}_{n+2},\ldots) = \lim_{k\to\infty} \frac{\mu_\varepsilon(V_{\underline{\sigma}_n\underline{\sigma}_{n+1}\cdots\underline{\sigma}_k})}{\mu_\varepsilon(V_{\underline{\sigma}_{n+1}\cdots\underline{\sigma}_k})} = \frac{h_{\underline{\sigma}_n\underline{\sigma}_{n+1}}}{h_{\underline{\sigma}_{n+1}\underline{\sigma}_{n+2}}} \frac{p_{\underline{\sigma}_n\underline{\sigma}_{n+1}}}{\alpha} \tag{51}$$

where the representation (48) of the measure has been used. Since the explicit form of the eigenvector of the transfer matrix is involved the corresponding stochastic spin dynamics is already fairly complicated. Thus we do not pursue this approach here.

Our model system shows that based on symbolic dynamics it is indeed possible to identify a qualitative change in the dynamics which appears only in the limit of infinite system size. By construction the type of phase transition described here is contained in the Ising universality class. For different choices of the single site map and the local slopes (42) quite general Hamiltonians can be realised. Thus different types of equilibrium phase transitions may appear in these models. One should however keep in mind that the approach requires to some extent a simple symbolic dynamics, since the influence of a complicated grammar on the phase transition behaviour is still unexplored.

3 Coupled Map Lattices and Kinetic Ising Models

The concept described in the previous section mainly focuses on stationary properties of dynamical systems like invariant measures or (stationary) correlation functions. Transient dynamics like relaxation towards equilibrium is difficult to tackle within such an approach. In contrast, coarse grained descriptions of the dynamics in terms of suitable partitions of phase space that keep the time as a dynamical variable are useful to cope with such problems. We will sketch that such ideas are capable to deal with the dynamics of coupled map lattices from a different perspective.

For the purpose of illustration let us consider a spatially one–dimensional coupled map lattice with single site maps motivated by the Miller–Huse model, cf. section 1. Hence we take the following double tent map defined on $I = [-1, 1]$ (cf. figure 8)

$$f_\delta(x) = \begin{cases} -2 - x/a & \text{if } -1 \le x \le -a \\ x/a & \text{if } -a < x < a \\ 2 - x/a & \text{if } a \le x \le 1 \end{cases} \tag{52}$$

where $1/a = 2 - \delta$ denotes the modulus of the slope. We introduce a small parameter $|\delta| \ll 1$ which will be useful later on for applying some analytical expansion. For $\delta = 0$ the two subintervals $I_+ = [0, 1]$ and $I_- = [-1, 0]$ are invariant sets. The single site map induces a hopping between these two intervals if $\delta < 0$ while hopping is suppressed for $\delta > 0$. On the level of a coarse grained description in terms of symbols $\sigma_n = \text{sign}(x_n)$ the motion may be considered as a kinetic single spin model. The transition emerging at $\delta = 0$ is a plain bifurcation, a so called crises [46], and the motion for $\delta < 0$ is usually called crisis induced intermittency. Nothing like a proper phase transition takes place at $\delta = 0$.

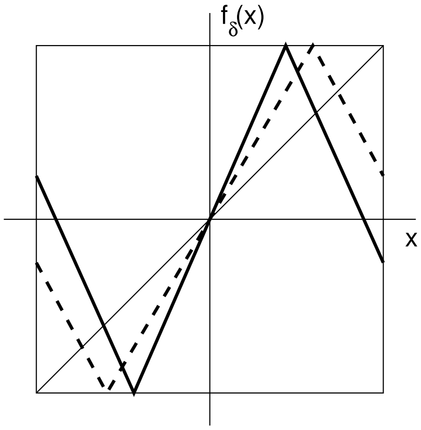

Fig. 8. Single site map, eq.(52), for two different values of the parameter δ. Solid line: $\delta < 0$, broken line $\delta > 0$.

Placing these maps on a chain of length L, introducing the nearest neighbour coupling (1a), and choosing periodic boundary conditions we obtain a kind of minimal model [21]

$$x_{n+1}^{(\nu)} = (T_{\varepsilon,\delta}(\underline{x}_n))^{(\nu)} = (1-\varepsilon) f_\delta(x_n^{(\nu)}) + \frac{\varepsilon}{2}\left[f_\delta(x_n^{(\nu+1)}) + f_\delta(x_n^{(\nu-1)})\right] \quad . \quad (53)$$

It is our goal to analyse the dynamics of eq.(53) using perturbation expansions for small $|\delta|$ and ε. Thus let us first comment on the trivial case $\delta = \varepsilon = 0$. Then each cube

$$I_{\underline{\sigma}} = I_{\sigma^{(0)}} \times I_{\sigma^{(1)}} \times \ldots \times I_{\sigma^{(L-1)}} \quad (54)$$

labelled by a symbol string $\underline{\sigma} = (\sigma^{(0)}, \ldots, \sigma^{(L-1)}) \in \{-,+\}^L$ is an invariant set with respect to the uncoupled map lattice $T_{\varepsilon=0,\delta=0}$. The dynamics in each cube is mixing. If we turn on the coupling and the deformation parameter δ transitions between the cubes may be induced. For instance considering an ensemble of initial conditions it seems tempting to describe the motion on a coarse grained level by the probability $p_n(\underline{\sigma})$ that at time n the trajectory visits cube $I_{\underline{\sigma}}$. Based on quite general arguments one may conclude that these probabilities obey a master equation

$$p_{n+1}(\underline{\sigma}) = p_n(\underline{\sigma}) + \sum_{\underline{\tilde{\sigma}}} \left[w(\underline{\tilde{\sigma}} \to \underline{\sigma}) p_n(\underline{\tilde{\sigma}}) - w(\underline{\sigma} \to \underline{\tilde{\sigma}}) p_n(\underline{\sigma})\right] \quad . \quad (55)$$

Formal derivations of such an equation from first principles can be obtained e.g. by applying standard projection operator techniques borrowed from nonequilibrium statistical physics [47, 48]. As for the structure of the master equation (55) we just recall that the two contributions in the sum just yield the gain and the loss due to transitions. The transition $\underline{\sigma} \to \underline{\sigma}$ drops from our considerations. For large n the solution of eq.(55) tends towards a stationary state $p_*(\underline{\sigma})$ which in fact may be identified with $\mu(I_{\underline{\sigma}})$ when μ denotes the SRB measure of the coupled map lattice. The essential approximation in writing down eq.(55) consists in neglecting non–Markovian contributions. Since in the perturbative regime $|\delta|, \varepsilon \ll 1$ transitions between different cubes are rare, the mixing dynamics in each cube ensures that the memory between different transitions is destroyed and the Markovian approach in terms of eq.(55) becomes feasible. The essential step remains to be the evaluation of the transition probabilities $w(\underline{\sigma} \to \underline{\tilde{\sigma}})$ quantifying transitions from cube $I_{\underline{\sigma}}$ to cube $I_{\underline{\tilde{\sigma}}}$.

Let us emphasise the difference between the present concept and the approach used previously in section 2. The description in terms of the master equation (55) relies on a spatial coarse graining of the dynamics. We do not require that the partition in terms of the cubes (54) fulfills some Markov property. Hence we do not resolve finer scales in phase space in terms of cylinder sets (cf. eq.(46)). Thus the probabilities $p_n(\underline{\sigma})$ are not capable to resolve the statistics within a cube. But the approach via eq.(55) still contains the time as a dynamical variable and thus can deal explicitly with transient dynamics and the relaxation towards equilibrium.

We are now going to estimate the transition probability for a fixed transition $\underline{\sigma} \to \underline{\tilde{\sigma}}$ in the limit of small coupling and deformation δ. Actually we will introduce a suitable notion for a transition so that finally the master equation is valid. The obvious definition $\underline{x}_n \in I_{\underline{\sigma}}$, $\underline{x}_{n+1} \in I_{\underline{\tilde{\sigma}}}$ fails since it does not refer to the time scale separation which accounts for the validity of the Markov approximation. In the perturbative regime transitions are rare as the trajectory spends most time in the interior of a cube. Let us assume that a particular coordinate $x^{(\nu)}$ at a fixed lattice site ν is going to change sign, i.e. it is going to induce the transition. Then depending on $\sigma^{(\nu)} = \mathrm{sign}(x^{(\nu)})$ the coordinate is either close to the maximum or to the minimum of the single site map

$$x^{(\nu)} = a\sigma^{(\nu)} + \mathcal{O}(\varepsilon, \delta) \tag{56}$$

since f_δ maps such points to the boundary of the interval $I_{\sigma^{(\nu)}}$ (cf. figure 8). Let us compute successive iterates up to first order in the small parameters ε and δ. Applying eq.(53) and taking into account that to first order $f_\delta(x^{(\nu)}) = (1 - 2|x^{(\nu)} - a\sigma^{(\nu)}|)\sigma^{(\nu)}$ we obtain for the first iterate at the site ν and its two neighbours

$$\begin{aligned}(T_{\varepsilon,\delta}(\underline{x}))^{(\nu)} = \sigma^{(\nu)} - \sigma^{(\nu)} \left(\varepsilon + 2|x^{(\nu)} - a\sigma^{(\nu)}|\right) \\ + \frac{\varepsilon}{2} \sum_{\rho=\pm 1} f_0(x^{(\nu+\rho)}) + \mathcal{O}(\varepsilon^2, \varepsilon\delta, \delta^2)\end{aligned} \tag{57}$$

and

$$(T_{\varepsilon,\delta}(\underline{x}))^{(\nu\pm1)} = f_0(x^{(\nu\pm1)}) + \mathcal{O}(\varepsilon,\delta) \quad . \tag{58}$$

Observing that the coordinate (57) is close to the boundary a similar computation yields for the second iterate

$$\begin{aligned}\left(T^2_{\varepsilon,\delta}(\underline{x})\right)^{(\nu)} &= \sigma^{(\nu)}\left(\delta + 2\varepsilon + 4|x^{(\nu)} - a\sigma^{(\nu)}|\right) \\ &\quad - \varepsilon \sum_{\rho=\pm1}\left[f_0(x^{(\nu+\rho)}) - \frac{1}{2}f_0^2(x^{(\nu+\rho)})\right] + \mathcal{O}(\varepsilon^2,\varepsilon\delta,\delta^2)\end{aligned} \tag{59}$$

and

$$\left(T^2_{\varepsilon,\delta}(\underline{x})\right)^{(\nu\pm1)} = f_0^2(x^{(\nu\pm1)}) + \mathcal{O}(\varepsilon,\delta) \quad . \tag{60}$$

Proceeding in the same way we obtain for the ℓth iterate

$$\begin{aligned}\left(T^\ell_{\varepsilon,\delta}(\underline{x})\right)^{(\nu)} &= 2^{\ell-2}\sigma^{(\nu)}\Big(\delta + 2\varepsilon + 4|x^{(\nu)} - a\sigma^{(\nu)}| \\ &\quad - \varepsilon\sigma^{(\nu)}\sum_{\rho=\pm1}\left[f_0(x^{(\nu+\rho)}) - 2t_\ell(x^{(\nu+\lambda)})\right]\Big) + \mathcal{O}(\varepsilon^2,\varepsilon\delta,\delta^2)\end{aligned} \tag{61}$$

where

$$t_\ell(x) = \sum_{k=2}^{\ell}\frac{1}{2^k}f_0^k(x) \quad . \tag{62}$$

Eq.(61) describes the asymptotic growth of the coordinate $x^{(\nu)}$ as long as its value stays in $[-a,a]$. From the definition (62) it is clear that the function t_ℓ approaches rapidly the limit

$$t_\infty(x) = \lim_{\ell\to\infty} t_\ell(x) \tag{63}$$

which is frequently called the Takagi function (cf. figure 9). Hence using this asymptotic property the coordinate $x^{(\nu)}$ changes sign from $\sigma^{(\nu)}$ to $-\sigma^{(\nu)}$ if

$$\delta + 2\varepsilon + 4|x^{(\nu)} - a\sigma^{(\nu)}| - \varepsilon\sigma^{(\nu)}\sum_{\rho=\pm1}\left[f_0(x^{(\nu+\rho)}) - 2t_\infty(x^{(\nu+\rho)})\right] < 0 \quad . \tag{64}$$

Thus the condition for the occurrence of a transition just depends on the neighbouring coordinates[15], i.e. on the nearest neighbour symbols $\sigma^{(\nu\pm1)}$. According to this observation the transitions can be grouped into three distinct types

type I:	$+\,+\,+ \to +\,-\,+$	$-\,-\,- \to -\,+\,-$	(65a)
type II:	$-\,+\,+ \to -\,-\,+$	$+\,-\,- \to +\,+\,-$	(65b)
type III:	$+\,-\,+ \to +\,+\,+$	$-\,+\,- \to -\,-\,-$	(65c)

[15]In higher orders of the perturbation expansion other lattice sites will enter as well.

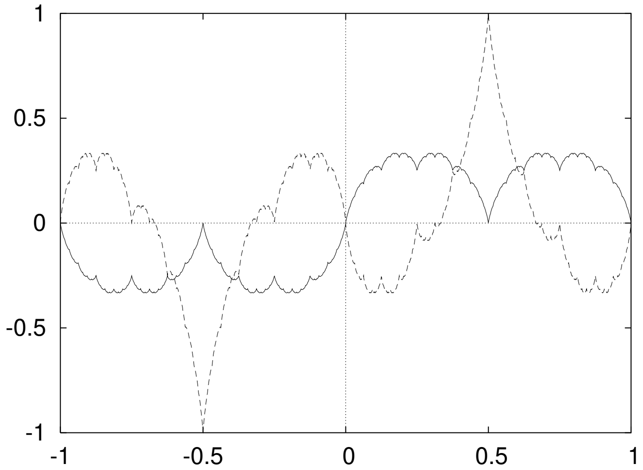

Fig. 9. Solid line: Takagi function $t_\infty(x)$, eq.(63). Broken line: $f_0(x) - 2t_\infty(x)$ (cf. eqs.(66) and (68)).

Only those transitions $\underline{\sigma} \to \underline{\tilde{\sigma}}$ enter the master equation (55) where a single symbol of the chain $\underline{\sigma}$ is flipped. Master equations with such special transition probabilities are often called kinetic Ising models. The dynamics of such an equation can be generated in terms of a stochastic spin dynamics according to the (local) transition rates of the master equation [49, 50]. Therefore even numerical simulations become feasible. They are widely used in the context of solid state physics.

The condition (64) determines which type of transition (65) is really possible and enters the sum in eq.(55) with finite probability. Obviously the optimal choice to fulfil the condition (64) is given by $x^{(\nu)} = a\sigma^{(\nu)}$ indicating that the transition starts in the centre of the interval. Optimal choices for the nearest neighbour coordinates have to maximise the expression containing the Takagi function, subjected to the constraint which type of transition is considered, i.e. which values for the nearest neighbour symbols $\sigma^{(\nu\pm1)} = \mathrm{sign}(x^{(\nu\pm1)})$ are assumed. Introducing the abbreviations

$$b_+ = \sup\{f_0(x) - 2t_\infty(x) \,|\, x \in [0,1]\} \tag{66a}$$
$$b_- = \sup\{f_0(x) - 2t_\infty(x) \,|\, x \in [-1,0]\} \tag{66b}$$

the condition (64) yields the constraints

$$\text{type I:} \qquad \delta < -2\varepsilon + 2\varepsilon b_+ \tag{67a}$$
$$\text{type II:} \qquad \delta < -2\varepsilon + \varepsilon(b_+ + b_-) \tag{67b}$$
$$\text{type III:} \qquad \delta < -2\varepsilon + 2\varepsilon b_- \tag{67c}$$

The numerical values of the constants (66) are computed straightforwardly by employing the self similar features of the Takagi function (cf. figure 9)

$$b_+ = 1, \qquad b_- = 1/3 \quad . \tag{68}$$

Hence the conditions (67) split the ε–δ parameter plane into four regions where different types of transitions occur (cf. figure 10 and [21] for a detailed analysis of the underlying kinetic Ising model):

- Region 1 ($\delta > 0$): According to eqs.(67) and (68) no transition is possible. No spin flips occur, i.e. all transition probabilities of the master equation (55) vanish. Each cube $I_{\underline{\sigma}}$ contains an attractor of the coupled map lattice.
- Region 2 ($-2\varepsilon/3 < \delta < 0$): Only transitions of type I are permitted. Those cubes $I_{\underline{\sigma}}$ contain an attractor where the symbol chain $\underline{\sigma}$ does not contain three successive symbols of the same type.
- Region 3 ($-4\varepsilon/3 < \delta < -2\varepsilon/3$): Transitions of type I and II are permitted. The dynamics settles on an alternating symbol sequence $\underline{\sigma} = (+,-,+,-,\ldots)$ or $\underline{\sigma} = (-,+,-,+,\ldots)$, if we consider for simplicity systems of even system size L. Thus there are two attractors
- Region 4 ($\delta < -4\varepsilon/3$): All types of transitions are feasible and the attractor encompasses all cubes.

Roughly speaking, decreasing δ increases the number of possible transitions and decreases the number of attractors of the coupled map lattice. One should however keep in mind that these changes are just plain bifurcations which change the topology in the phase space. They are not linked to (proper) phase transitions as the size of the system does not play an essential role.

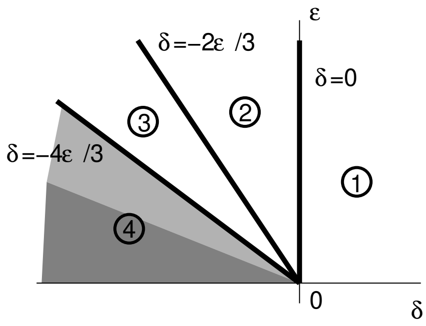

Fig. 10. Diagrammatic view of the bifurcation diagram of the coupled map lattice (53) according to the conditions (67). Labels refer to the regions mentioned in the text. Greyshading indicates the type of coupling according to eq.(72), antiferromagnetic (light), ferromagnetic (dark).

While we have so far discussed which transition is possible we may in addition estimate the numerical value of the corresponding transition probability. Condition (64) determines those points in the phase space which trigger a particular transition

$$E_{\sigma^{(\nu-1)},\sigma^{(\nu)},\sigma^{(\nu+1)}} = \{(x^{(\nu-1)}, x^{(\nu)}, x^{(\nu+1)}) \in I_{\sigma^{(\nu-1)}} \times I_{\sigma^{(\nu)}} \times I_{\sigma^{(\nu+1)}} \mid$$
$$\delta + 2\varepsilon + 4|x^{(\nu)} - a\sigma^{(\nu)}| - \varepsilon\sigma^{(\nu)} \sum_{\rho=\pm 1} \left[f_0(x^{(\nu+\rho)}) - 2t_\infty(x^{(\nu+\rho)}) \right] < 0\} \quad (69)$$

Assuming that due to the mixing properties of the tent map and the small transitions rates the distribution of phase space points stays uniform within each cube we may estimate the transition rate by the (normalised) volume of the transition region (69). The numerical values of the transition rates determine the dynamics of the corresponding kinetic Ising model. Here we focus on the behaviour in region 4 and refer the interested reader for the discussion of the other cases to the literature [21]. In region 4 all three types of transitions (67) are possible with finite transition rates w_I, w_{II} and w_{III}. Actually we have obtained a kinetic Ising model with nearest neighbour interaction (cf. [49]). For the stationary distribution the sum in the master equation (55) must vanish. In our case the even stronger condition of detailed balance holds meaning that each term of the sum vanishes individually[16]

$$w(\underline{\tilde{\sigma}} \to \underline{\sigma}) p_*(\underline{\tilde{\sigma}}) - w(\underline{\sigma} \to \underline{\tilde{\sigma}}) p_*(\underline{\sigma}) = 0 \quad . \quad (70)$$

Observing that transitions of type II do not increase the number of $+/-$ pairs in the symbol chain, and that transitions of type I and III are inverse to each other one easily recognises that the stationary solution can be written as

$$p_*(\underline{\sigma}) = \frac{1}{Z} \exp\left(J \sum_{\nu=0}^{L-1} \sigma^{(\nu)} \sigma^{(\nu+1)} \right) \quad (71)$$

when we define the effective exchange constant by the ratio of the transition probabilities

$$J = \frac{1}{4} \ln\left(\frac{w_{III}}{w_I} \right) \quad . \quad (72)$$

In fact, the validity of eqs.(70), (71), and (72) is easily checked a posteriori. Close to the boundary of region 3 the transition rate w_{III} is small and the coupling (72) is predominantly antiferromagnetic, in accordance with the stationary state in region 3. Within region 4 w_{III} may increase and the coupling may turn out to become ferromagnetic (cf. figure 10). Above all the stationary state in region 4 is a finite temperature canonical ensemble of an Ising chain. Of course no phase transition will occur in this one–dimensional setup.

Since the one–dimensional coupled map lattice (53) can be described in terms of a one–dimensional kinetic Ising model it seems tempting to investigate (proper) phase transitions by considering the spatially two–dimensional case. But here one has to add an important reservation. The analysis of the

[16] Actually this condition poses a constraint on the transition probabilities in terms of a potential condition [51].

model (53) resulted in a coarse grained description which obeys detailed balance (70). Such a condition requires constraints on the transition rates which crucially depend on the underlying coupled map lattice. Taking for instance a one–dimensional coupled map lattice with asymmetric coupling, one obtains transition rates violating detailed balance (cf. [52] for the analysis of the unidirectionally coupled case). Thus in general one may end up with nonequilibrium kinetic Ising models. In such cases phase transitions are possible even in the spatially one–dimensional setup [53]. A similar phenomenon occurs for the obvious generalisation of the model (53) to two spatial dimensions. Again one obtains a master equation violating detailed balance. Thus a proper understanding of phase transitions in coupled map lattices calls for a deeper understanding of nonequilibrium models in statistical mechanics. In fact, as proven in [6] one may end up with a coarse grained description which is more general than a kinetic Ising model. In such cases one has to introduce carefully the concept of a (proper) phase transition since the notions form equilibrium statistical mechanics do not apply directly. Above all more research even for quite simple models is still needed in order to classify phase transitions in coupled map lattices properly.

References

1. M. C. Cross and P. C. Hohenberg, *Pattern–formation outside of equilibrium*, Rev. Mod. Phys. **65**, 851 (1993).
2. J. P. Crutchfield and K. Kaneko, in *Directions in Chaos*, edited by H. Bai-Lin (World Scientific Publ., Singapore, 1987), p. 272.
3. K. Kaneko, *Pattern dynamics in spatiotemporal chaos*, Physica D **34**, 1 (1989).
4. J. Guckenheimer and P. Holmes, *Nonlinear Oscillations, Dynamical Systems, and Bifurcations of Vector Fields* (Springer, New York, 1986).
5. H. Haken, *Synergetics* (Springer, Berlin, 1977).
6. G. Gielis and R. S. MacKay, *Coupled map lattices with phase transition*, Nonlin. **13**, 867 (2000).
7. K. Kaneko, *Theory and applications of coupled map lattices* (Wiley, Chichester, 1993).
8. L. A. Bunimovich and Y. G. Sinai, *Spacetime chaos in coupled map lattices*, Nonlin. **1**, 491 (1988).
9. J. Bricmont and A. Kupiainen, *Coupled analytic maps*, Nonlin. **8**, 379 (1995).
10. C. Maes and A. V. Moffaert, *Stochastic stability of weakly coupled lattice maps*, Nonlin. **10**, 715 (1997).
11. T. Fischer and H. H. Rugh, *Transfer operators for coupled analytic maps*, Erg. Theor. Dyn. Syst. **20**, 109 (2000).
12. *Collective dynamics of nonlinear and disordered systems*, edited by G. Radons, P. Häussler, and W. Just (Springer, Berlin, 2004).
13. K. Kaneko, *Mean field fluctuation of a network of chaotic elements*, Physica D **55**, 368 (1992).
14. K. Kaneko, *Globally coupled chaos violates the law of large numbers but not the central–limit theorem*, Phys. Rev. Lett. **65**, 1391 (1990).

15. E. Järvenpää, *A SRB–measure for globally coupled circle maps*, Nonlin. **10**, 1435 (1997).
16. S. V. Ershov and A. B. Potapov, *On the mean field fluctuations in globally coupled maps*, Physica D **86**, 523 (1995).
17. T. Chawanya and S. Morita, *On the bifurcation structure of the mean–field fluctuation in the globally coupled tent map system*, Physica D **116**, 44 (1998).
18. G. Keller, *An ergodic theoretic approach to mean field coupled maps*, Prog. Prob. **46**, 183 (2000).
19. W. Just, *Globally coupled maps: phase transitions and synchronization*, Physica D **81**, 317 (1995).
20. K. Kaneko, *Supertransients, spatiotemporal intermittency and stability of fully developed spatiotemporal chaos*, Phys. Lett. A **149**, 105 (1990).
21. F. Schmüser, W. Just, and H. Kantz, *On the relation between coupled map lattices and kinetic Ising models*, Phys. Rev. E **61**, 3675 (2000).
22. J. Miller and D. A. Huse, *Macroscopic equilibrium from microscopic irreversibility in a chaotic coupled map lattice*, Phys. Rev. E **48**, 2528 (1993).
23. H. Sakaguchi, *Phase transition in coupled Bernoulli maps*, Prog. Theor. Phys. **80**, 7 (1988).
24. P. Marcq, H. Chaté, and P. Manneville, *Universality in Ising–like phase transitions of coupled chaotic maps*, Phys. Rev. E **55**, 2606 (1997).
25. A. Lemaître and H. Chaté, *Phase ordering and onset of collective behavior in chaotic coupled map lattices*, Phys. Rev. Lett. **82**, 1140 (1999).
26. X. J. Wang, *Statistical physics of temporal intermittency*, Phys. Rev. A **40**, 6647 (1989).
27. C. S. Hsu, *Cell–to–cell mapping : a method of global analysis for nonlinear systems* (Springer, New York, 1987).
28. M. Dellnitz, A. Hohmann, O. Junge, and M. Rumpf, *Exploring invariant sets and invariant measures*, Chaos **7**, 221 (1997).
29. M. Dörfle, *Spectrum and eigenfunctions for the Frobenius–Perron operator of the tent map*, J. Stat. Phys. **40**, 93 (1985).
30. S. Morita, *Bifurcations in globally coupled chaotic maps*, Phys. Lett. A **211**, 258 (1996).
31. C. Beck and F. Schlögl, *Thermodynamics of chaotic systems* (Cambridge University Press, Cambridge, 1995).
32. W. Just, in *Collective dynamics of nonlinear and disordered systems*, edited by G. Radons, P. Häussler, and W. Just (Springer, Berlin, 2004).
33. K. Falconer, *Techniques in fractal geometry* (Wiley, Chicester, 1997).
34. A. Lasota and M. C. Mackey, *Chaos, Fractals, and Noise: Stochastic Aspects of Dynamics* (Springer, New York, 1994).
35. H. Mori, B. S. So, and T. Ose, *Time–correlation functions of one–dimensional transformations*, Prog. Theor. Phys. **66**, 1266 (1981).
36. T. Bohr and D. Rand, *The entropy function for characteristic exponents*, Physica D **25**, 387 (1987).
37. G. Pianigiani and J. A. Yorke, *Expanding maps on sets which are almost invariant: Decay and chaos*, Trans. Amer. Math. Soc. **252**, 351 (1979).
38. R. Bowen, in *Equilibrium States and the Ergodic Theory of Anosov Diffeomorphisms*, Vol. 470 of *Lecture Notes in Mathematics*, edited by A. Dold and B. Eckmann (Springer, Berlin, 1975).

39. T. C. Halsey, M. H. Jensen, L. P. Kadanoff, I. Procaccia, and B. I. Shraiman, *Fractal measures and their singularities: The characterization of strange sets*, Phys. Rev. A **33**, 1141 (1986).
40. P. Grassberger, R. Badii, and A. Politi, *Scaling laws for invariant measures on hyperbolic and nonhyperbolic attractors*, J. Stat. Phys. **51**, 135 (1988).
41. W. Just and H. Fujisaka, *Gibbs Measures and Power Spectra for Type I Intermittent Maps*, Physica D **64**, 98 (1993).
42. C. Robinson, *Dynamical systems : stability, symbolic dynamics, and chaos* (CRC Press, Boca Raton, 1995).
43. R. Artuso, E. Aurell, and P. Cvitanović, *Recycling of strange sets*, Nonlin. **3**, 325 (1990).
44. D. Ruelle, *Thermodynamic formalism* (Addison-Wesley, Reading, 1978).
45. W. Just, *Equilibrium phase transitions in coupled map lattices: a pedestrian approach,*, J. Stat. Phys. **105**, 133 (2001).
46. C. Grebogi, E. Ott, and J. A. Yorke, *Crisis sudden changes in chaotic attractors and transient chaos*, Physica D **7**, 181 (1983).
47. E. Fick and G. Sauermann, *The quantum statistics of dynamic processes* (Springer, Berlin, 1990).
48. W. Just, *Projection operator approach to the thermodynamic formalism of dynamical systems*, J. Stat. Phys. **67**, 271 (1992).
49. R. J. Glauber, *Time–dependent statistics of the Ising model*, J. Math. Phys. **4**, 294 (1963).
50. K. Kawasaki, in *Phase Transitions and Critical Phenomena*, edited by C. Domb (Academic Press, London, 1972), p. 443.
51. F. P. Kelly, *Reversibility and Stochastic Networks* (Wiley, Chichester, 1979).
52. F. Schmüser and W. Just, *Non–equilibrium behaviour in unidirectionally coupled map lattices*, J. Stat. Phys. **105**, 525 (2001).
53. *Nonequilibrium Statistical Mechanics in One Dimension*, edited by V. Privman (Cambridge University Press, Cambridge, 1997).

Index

bifurcation, 2
bifurcation diagram, 28

Cantor set, 10, 16
coarse grained description, 7, 23
coupled maps
  globally, 4
  random, 4
  weakly, 7
coupling function, 3
cylinder set, 10, 18, 21

detailed balance, 29
  violation of, 30
diffusive coupling, 3

equilibrium phase transition, 2, 7
ergodic component, 7, 22
escape factor, 12

fractal, 16
Frobenius–Perron equation, 12

high–temperature phase, 7

intermittency, 15, 17
invariant measure, 11, 19, 21
  conditional, 12
Ising model
  kinetic, 6, 8, 24, 27, 29
  nonequilibrium, 30
  one–dimensional, 17, 29
  two–dimensional, 6, 8, 22
iterated function scheme, 8, 15

local expansion rate, 22
localisation, 22

Markov approximation, 25
Markov chain, 16
Markov partition, 11
master equation, 24
Miller–Huse model, 6
mixing
  spatio–temporal, 7
multifractal, 14

partition, 7, 21, 25
pattern formation, 1
piecewise linear map, 9

repeller, 10, 12

short range interaction, 15
space–time chaos, 1, 4
spatio–temporal dynamics, 1
spin Hamiltonian, 14, 20, 22
spin lattice, 19
SRB measure, 14
statistical mechanics, 7, 8, 15, 18
supertransients, 5
symbol shift, 10
symbolic dynamics, 7, 8

Takagi function, 26
thermodynamic limit, 4, 23
transfer matrix, 12
transient dynamics, 4
transition
  type I–III, 26
transition probability, 16, 25, 28